The Greenland Ice-Marginal Lake Inventory Series from 2016 to 2023

Penelope How, Dorthe Petersen, Nanna B. Karlsson, Kristian K. Kjeldsen, Katrine Raundrup, Alexandra Messerli, Anja Rutishauser, Jonathan L. Carrivick, James M. Lea, Robert S. Fausto, Andreas P. Ahlstrøm, Signe Bech Andersen

[1] Department of Glaciology and Climate, Geological Survey of Denmark and Greenland, Denmark

[2] Department of Hydrology and Climate, Asiaq Greenland Survey, Greenland

[3] Department of Environment and Minerals, Greenland Institute of Natural Resources, Greenland

[4] School of Geography and water@leeds, University of Leeds, UK

[5] Department of Geography and Planning, University of Liverpool, UK

Abstract

The Greenland ice sheet margin position, configuration and character is changing rapidly due to a variety of inter-linked processes ultimately forced by climate change. Understanding the influence of ice-marginal conditions, most especially transitions in environment from marine to land, or from land to lake, for example, on ice dynamics required an ice-marginal lake inventory series. Ice-marginal lakes also exert a profound control on downstream aquatic systems. Here, we provide eight annual records of lake abundance, surface extents, and surface water temperature estimates from 2016 to 2023. Ice-marginal lakes are defined as water bodies over 0.05 km² that share a boundary with the Greenland Ice Sheet or its surrounding ice caps and glaciers. (PGICs). Lakes were classified using a semi-automated multi-method remote sensing approach from Sentinel-1, Sentinel-2, and ArcticDEM data sources. The dataset catalogs 4543 ice-marginal lakes, with 2915±36% classified automatically and an average lake size of 1.29 km^2. This dataset fills critical gaps in understanding Greenland's terrestrial water storage and its implications for sea level rise, providing a first step toward quantifying meltwater storage at ice margins. It enables assessments of glacier dynamics, such as lacustrine-driven ablation, and supports Arctic ecological studies of lake changes impacting ecosystems. The inventory series also aids environmental management and hydropower planning aligned with Greenland's proposed commitments under the Paris Agreement. The series is openly accessible on the GEUS Dataverse (https://doi.org/10.22008/FK2/MBKW9N) with full metadata, documentation, and a reproducible processing workflow.

1. Introduction

The Greenland Ice Sheet and its surrounding ice caps and glaciers (PGICs) are forecast to be the largest cryospheric contributor to sea level rise over the coming century (AMAP, 2021). At present,

these projections assume that meltwater from the Ice Sheet flows directly into the ocean, but an increasing portion of this meltwater is stored temporarily in ice-marginal lakes along the ice margin (Shugar et al., 2020). The delayed release of meltwater at the ice margin is a significant, dynamic component of terrestrial storage (Sutherland et al., 2020). Ice-marginal lakes around the Greenland Ice Sheet form as meltwater becomes trapped at the terminus or edges of an outlet glacier (How et al., 2021; Carrivick et al., 2022). These lakes and be persistent and stable but an increasing number are recognised to be highly dynamic systems (Carrivick and Quincey, 2014), for example being prone to sudden and short-lived drainage producing GLOFs (Glacial Lake Outburst Flood events), which are also referred to as a *Jökulhlaup* (Icelandic) or *Sermimi supineq* (direct translation into Kalaallisut, West Greenlandic). GLOFs in Greenland have characteristics of megafloods (Carrivick and Tweed, 2019), have caused glacier speed-up events (e.g. Kjeldsen et al., 2017) and impacts on downstream erosion and sedimentation rates (e.g. Grinsted et al., 2017), and water salinity (e.g. Kjeldsen et al., 2014).

The presence of an ice-marginal lake introduces a suite of thermo-mechanical processes, including lacustrine submarine melting and calving (Zhang et al., 2023), that can dictate glacier margin morphology, dynamics and exacerbate ice mass loss Sutherland et al., 2020; Carrivick et al., 2020). At Russel Lake, situated beside Russel Glacier in Kangerlussuaq (West Greenland), these processes are relatively well-documented, illustrating how lake presence enhances melt-under-cutting and calving (Carrivick et al., 2017; Dømgaard et al., 2023). With continued retreat of the Greenland Ice Sheet under a warming climate, ice-marginal lakes and their associated processes are expected to become more abundant, larger, and warmer, which will likely amplify lacustrine-driven proglacial melt rates and GLOF events (Carrivick and Tweed, 2016; 2019; Grinsted et al., 2017; Shugar et al., 2020; Carrivick et al., 2023; Dye et al., 2021; Lützow, Veh and Korup, 2023; Rick et al., 2023; Veh et al., 2023; Holt et al., 2024; Zhang et al., 2024). However, ice-marginal lakes and their associated processes are largely absent from sea level change projections, which assume an immediate meltwater contribution to the ocean. This assumption overlooks the role of ice-marginal lakes as intermediary storage, and changes in lacustrine conditions, for instance when glaciers retreat onto land.

Mapping ice-marginal lakes is challenging due to the variability in lake characteristics. Remote sensing has been a viable approach for mapping the presence and surface extent of ice-marginal lakes, as demonstrated by inventories in Greenland (How et al., 2021), Alaska (Rick et al., 2022), Norway (Andreassen et al., 2022), Svalbard (Wieczorek et al., 2023) and High Mountain Asia (Chen et al., 2021). In general, classification approaches have been established to identify water bodies from SAR (Synthetic Aperture Radar) and multi-spectral (i.e. red, green, blue, near-infrared, shortwave) imagery, along with water potential identification using sink analysis from Digital Elevation Models (DEMs). As Greenland covers a large latitudinal range, ice-marginal lakes have very varying conditions which make them difficult to classify through one adopted method (How et al., 2021). For instance, surface sediment load, ice, and snow cover can vary significantly, with perennial ice cover in some cases at high latitudes and elevations (e.g. Mallalieu et al., 2021). Accordingly, multi-method classification approaches are necessary to capture this diversity (How et al., 2021).

Existing ice-marginal lake inventories are often static and therefore do not capture the dynamic nature of these lakes, nor capture new lakes and retire detached lakes once the margin has retreated. Given that ice-marginal lakes are projected to increase in size and abundance over time (Shugar et al., 2020; Zhang et al., 2024), it is of utmost importance to generate time-series that adequately capture ice-marginal lake change and assess the impact of these changes on future sea level projections.

Here, we present an annual series of Greenland ice-marginal lakes from 2016 to 2023, classified using an established multi-method remote sensing approach. Each annual inventory maps lake surface area and abundance, along with attributes such as known lake name and surface water temperature estimations. These inventories reveal evolving lake conditions that support future assessments of sea level contribution, ecosystem productivity, and biological activity associated with the Greenland Ice Sheet and the PGICs.

2. Data Description

2.1. Dataset overview

The annual inventory series is a natural follow-on from the 2017 Greenland ice-marginal lake inventory (How et al., 2021), largely adopting the same classification approach, data structure and formatting. The dataset consists of a series of annual inventories, mapping the extent and presence of ice-contact lakes across Greenland (Figure 1). Ice-contact lakes are defined as water bodies > 0.05 km^2, which are immediately adjacent to the Greenland Ice Sheet and/or the PGICs of Greenland. - Lake presence and outlines are provided, which denote the surface area as classified using a semi-automatic approach as described subsequently. The annual inventory series spans the entirety of Greenland, including all terrestrial regions. Thus far, there are 8 annual inventories, covering 2016 to 2023, where one inventory represents one year.

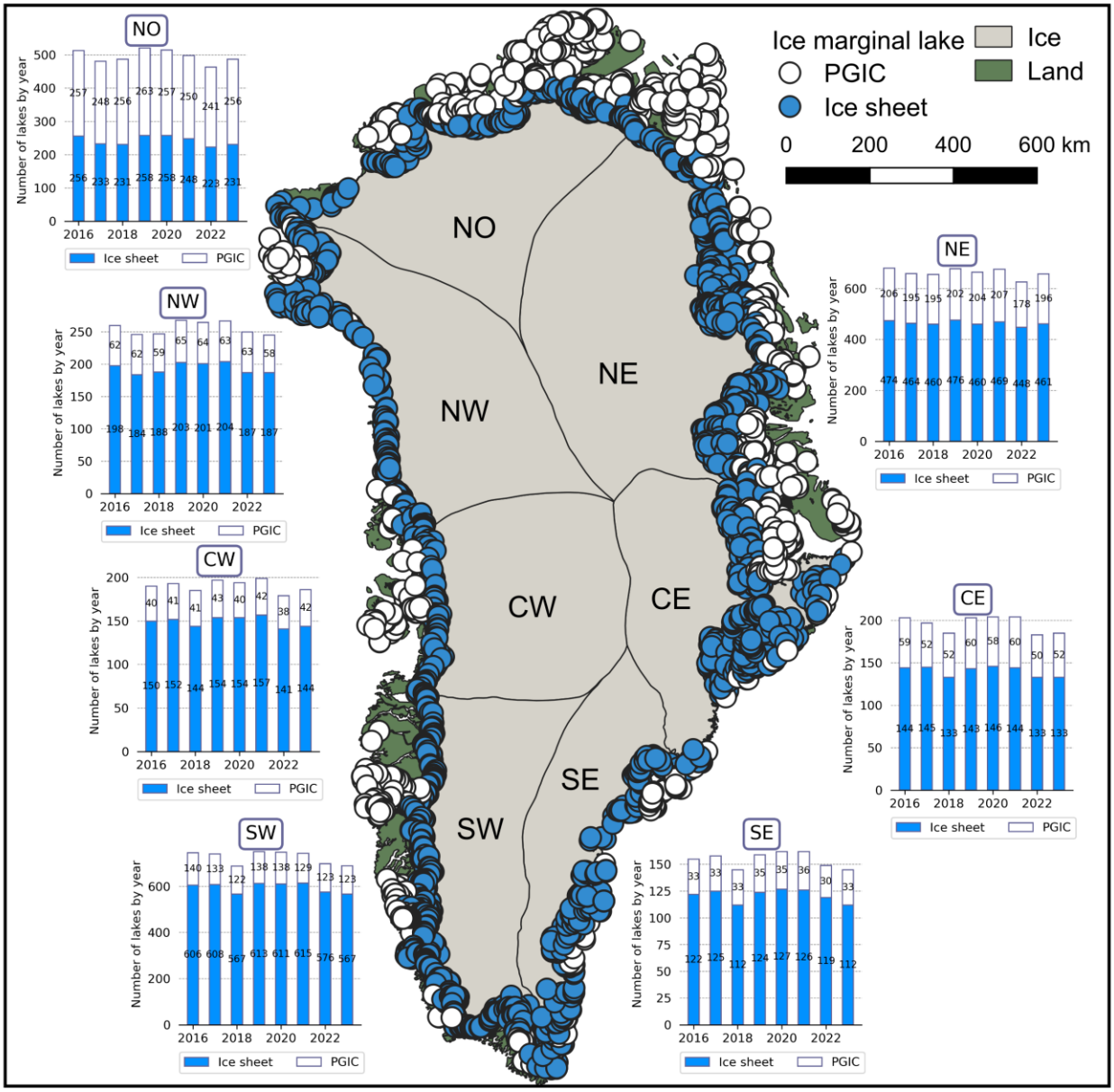

Figure 3. An overview of the ice-marginal lake inventory series, 2016-2023. Each mapped point denotes a unique lake, mapped across the Greenland Ice Sheet margin (blue) and the surrounding PGIC margins (white). The pie charts associated with each region shows the classification methodology performance, that being the number of lakes classified with the backscatter thresholding (SAR), multi-spectral classification (VIS) and sink detection (DEM) methods. The catchment regions are those defined by Mouginot and Rignot (2019). Base maps for plotting are from QGreenland v3.0 (Moon et al., 2023).

The dataset identifies 4543 ice-marginal lakes, with 2915±36% automatically delineated as part of the ice-marginal lake inventory series (Figure 1). Of these lakes, 2047±36% share a margin with the ice sheet whilst 868±36% are in contact with the PGICs. The largest lake in the inventory is Romer Sø, located in northeast Greenland, with a total area of 126.86 km^2. The average lake size is 1.29 km^2, and the median lake size is 0.28 km^2 with 2382 lakes between 0.05-1.00 km^2 (82%). Only 59 lakes in the inventory series have a total area above 10 km^2 (2%). The inventory series

also demonstrates changes to lake morphology (and the corresponding change in ice margin morphology), of which four example scenarios are presented in Figure 2. A classic terminus basin retreat style is evident across many ice-marginal lake extents, as presented in Fig. 2a, where terminus retreat/lake expansion is marked in the central section of the glacier outlet, leaving a trailing terminus morphology at the lateral margins. Peripheral terminus retreat is highlighted in Fig. 2b, where terminus retreat/lake expansion is focused at the lateral margins. There are rare instances where the presence of a lake affects the boundary conditions of two glacier termini, as demonstrated in Fig. 2c, where two glaciers terminate into the same common ice-marginal lake. And finally, there are instances displayed in the inventory series where there is margin retreat/lake expansion focused around a discrete zone, such as in Fig. 2d where a marked embayment has formed at a particular point in the north region of the glacier terminus.

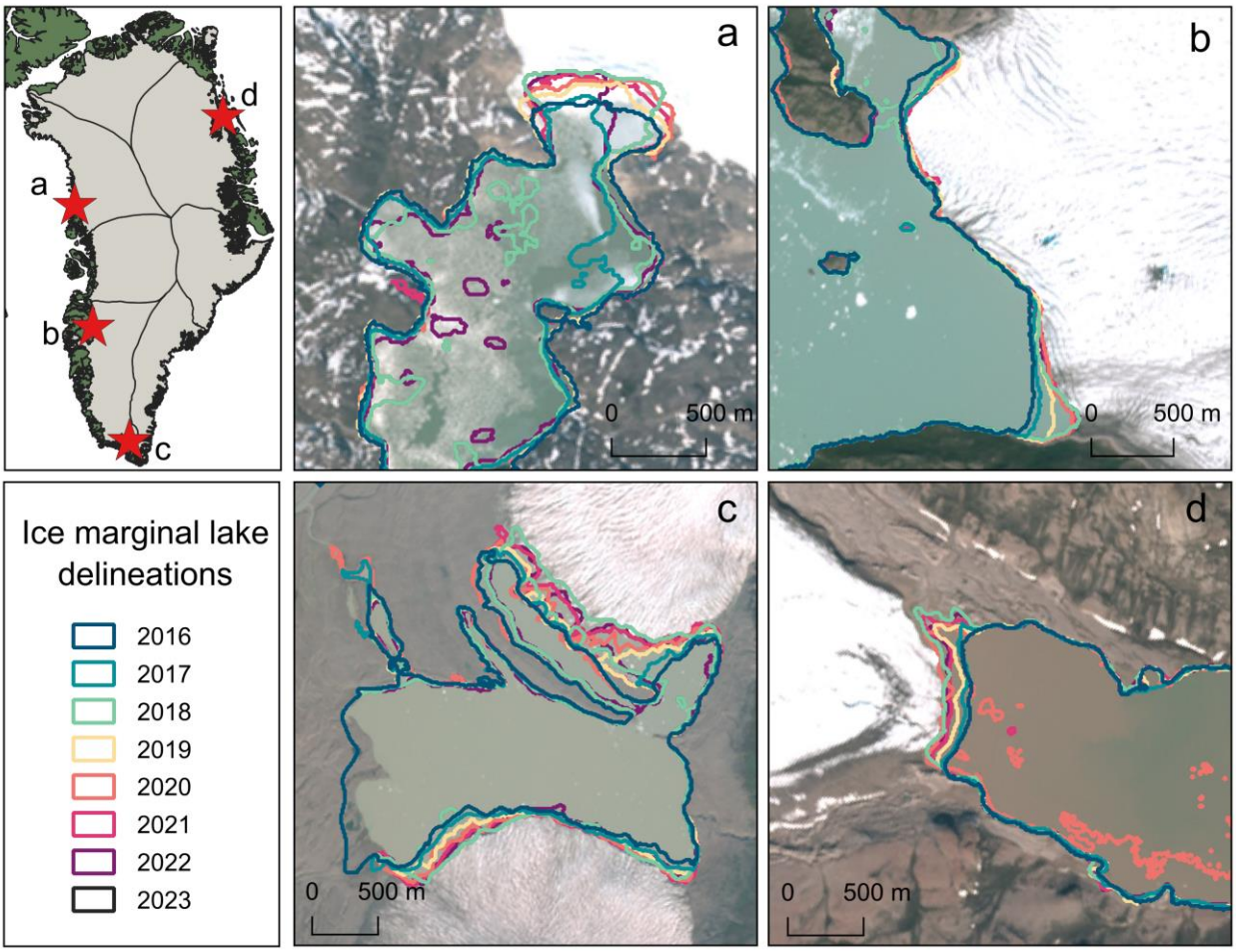

Figure 2. Examples of lake change, and the corresponding evolution of ice termini morphology, from the ice-marginal lake inventory series. These examples highlight basin margin retreat (a), peripheral margin retreat (b), bilateral margin retreat (c), and focused margin retreat (d). The background satellite imagery presented is from the Sentinel-2 10 m 2022 mosaic, produced by Styrelsen for Dataforsyning and Infrastruktur (2024). The base layers for the insert map plotting are from QGreenland v3.0 (Moon et al., 2023).

An average surface temperature estimate is derived for each inventory lake from all available Landsat 8/9 scenes acquired in the month of August for each inventory year. This information is provided in the metadata of the ice-marginal lake inventory series. A slight increase in surface lake temperature is evident, with the average lake surface temperature increasing from 5.78±0.88°C in 2016 to 6.16±0.88°C in 2023 (Figure 3). Fluctuations year on year vary, with instances of lake temperature falling between annual time steps (e.g. falling from 5.17±0.88°C to 4.44±0.88°C from 2017 to 208), rising (e.g. from 5.59±0.88°C to 6.16±0.88°C from 2022 to 2023), and remaining consistent (e.g. from 5.56 ± 0.88 °C to 5.5 9 ± 0.88 °C from 2021 to 2022).

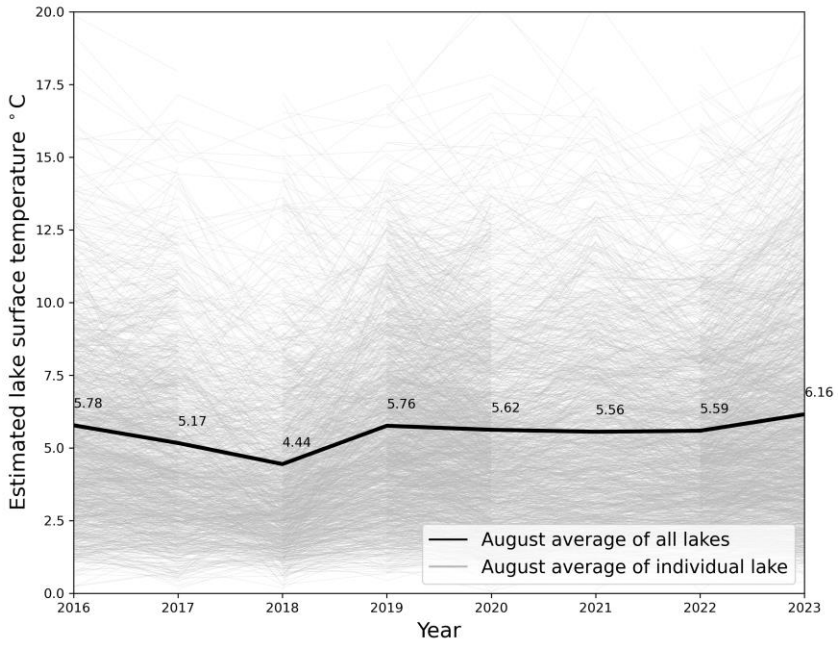

Figure 3. Average surface lake temperature estimates from the month of August at each inventory lake for each inventory year (2016-2023) (grey), with the average of all lakes overlaid (black). Surface lake temperature is derived from Landsat 8 and Landsat 9 OLI/TIRS Collection 2 Level 2 surface temperature data product. Averages are calculated from all available scenes acquired from the month of August to limit the risk of mis-estimates due to ice-covered conditions.

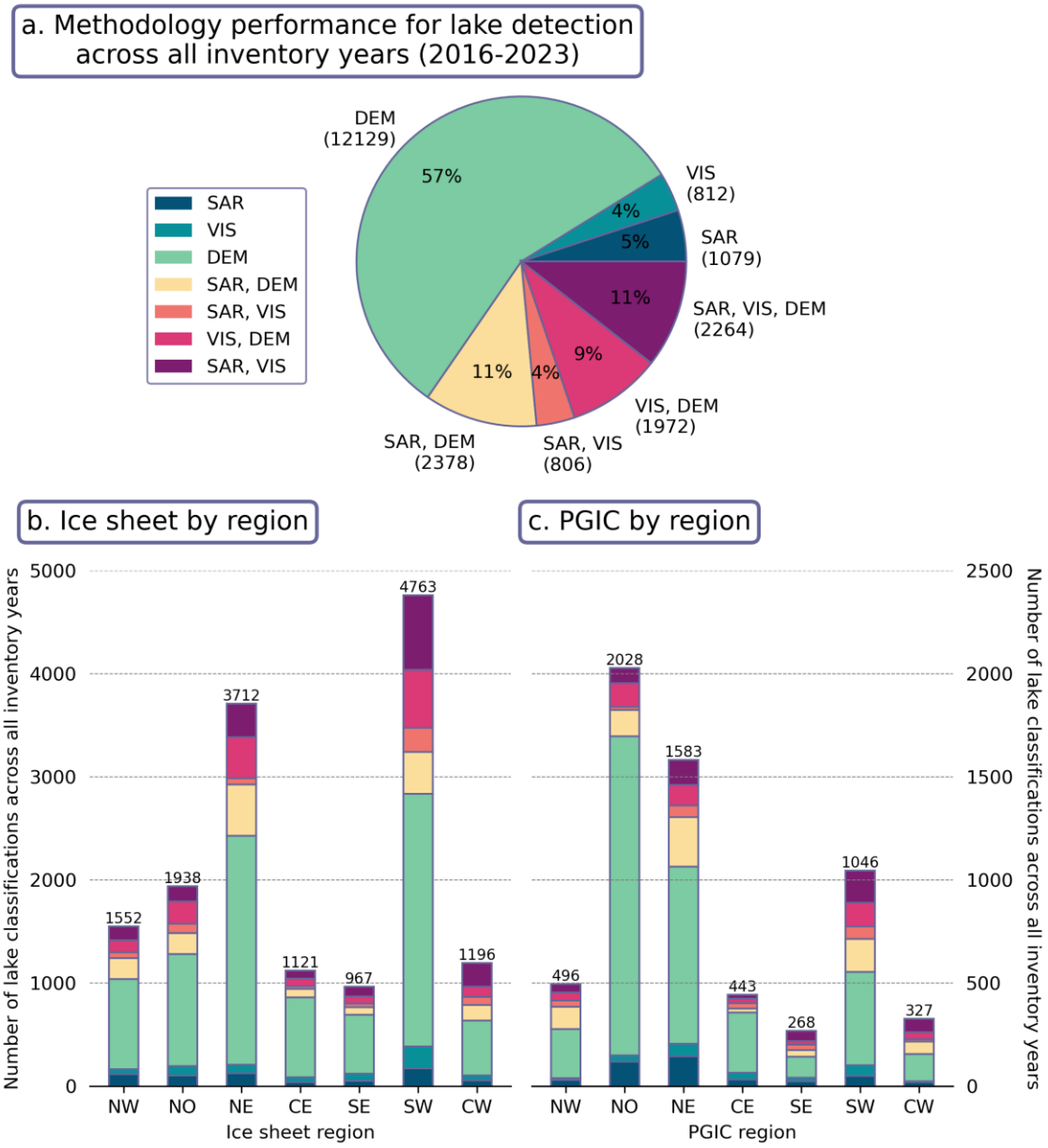

2.2. Data sources and acquisition

Ice-marginal lakes are identified using three established classification methods, from Synthetic Aperture Radar (SAR) and multi-spectral imagery, and Digital Elevation Models (DEMs). Classifications from SAR and multi-spectral imagery for each inventory year are identified from all available Sentinel-1 and Sentinel-2 image acquisitions for the months of July and August (Table 1). DEM classifications are made from a static data product which covers the period 2008 to 2016. Metadata for each identified lake includes a lake surface temperature estimate, which is derived from multi-spectral/infrared imagery.

Table 1. Summary of satellite data sources

Satellite	Data product	Acquisition filters	Spatial resolution
Sentinel-1	Ground Range Detected (GRD) dual-polarization C-band SAR images	Interferometric Wide Swath (IW) Horizontal-Horizontal (HH) polarisation 01 Jul to 31 Aug	10 metres
Sentinel-2	Multispectral instrument (MSI), Top of Atmosphere (TOA), Level 1C images	01 Jul to 31 Aug 20% max. cloud cover	10 metres
-	ArcticDEM mosaic (version 3)	-	2 metres
Landsat 8/9	Operational Land Imager/Thermal Infrared Sensor (OLI/TIRS), Collection 2, Level 2, surface temperature science product	01 to 31 Aug 30% max. cloud cover	30 metres

2.3. Data format and structure

The inventory series data are distributed as polygon vector features in shapefile format (.shp), with coordinates provided in the WGS NSIDC Sea Ice Polar Stereographic North (EPSG:3413) projected coordinate system. File names follow the convention defined in the original 2017 Greenland ice-marginal lake inventory (Wiesmann et al., 2021; How et al., 2021): *"<inventory-year>-<funder>-<project-acronym>-IML-f<version-number>.<file-extension>"*.

Each shapefile contains metadata regarding the lake description, physical measurements, lake surface temperature, method/s of classification, verification and possible editing (Table 2). A key piece of metadata to highlight is the lake identification number ("lake_id", Table 2), which are assigned to each classified ice-marginal lake, often consisting of multiple polygon features and/or classifications. These unique identifications are compatible across inventory years, therefore supporting time-series analysis and comparison across inventories.

Table 2. Summary of metadata included with each ice-marginal lake inventory in the annual series

Variable name	Description	Format
row_id	Index identifying number for each polygon	Integer
lake_id	Identifying number for each unique lake	Integer
lake_name	Lake placename, as defined by the Oqaasileriffik (Language Secretariat of Greenland) (https://oqaasileriffik.gl) placename database which is distributed with QGreenland (https://qgreenland.org/)	String
margin	Type of margin that the lake is adjacent to ("ICE_SHEET", "ICE_CAP")	String
region	Region that lake is located, as defined by Mouginot and Rignot (2019) ("NW", "NO", "NE", "CE", "SE", "SW", "CW")	String

area_sqkm	Areal extent of polygon/s in square kilometres	Float
length_km	Length of polygon/s perimeter in kilometres	Float
temp_aver	Average lake surface temperature estimate for the month of August (in degrees Celsius), derived from the Landsat 8/9 OLI/TIRS Collection 2 Level 2 surface temperature data product	Float
temp_min	Minimum pixel lake surface temperature estimate for the month of August (in degrees Celsius), derived from the Landsat 8/9 OLI/TIRS Collection 2 Level 2 surface temperature data product	Float
temp_max	Maximum pixel lake surface temperature estimate for the month of August (in degrees Celsius), derived from the Landsat 8/9 OLI/TIRS Collection 2 Level 2 surface temperature data product	Float
temp_stdev	Average lake surface temperature estimate standard deviation for the month of August, derived from the Landsat 8/9 OLI/TIRS Collection 2 Level 2 surface temperature data product	Float
method	Method of classification ("DEM", "SAR", "VIS")	String
source	Image source of classification ("ARCTICDEM", "S1", "S2")	String
all_src	List of all sources that successfully classified the lake (i.e. all classifications with the same "lake_name" value)	String
num_src	Number of sources that successfully classified the lake ("1", "2", "3")	Integer
certainty	Certainty of classification, which is calculated from "all_src" as a score between "0" and "1"	Float
start_date	Start date for classification image filtering	String
end_date	End date for classification image filtering	String
verified	Flag to denote if the lake has been manually verified ("Yes", "No")	String
verif_by	Author of verification	String
edited	Flag to denote if polygon has been manually edited ("Yes", "No")	String
edited_by	Author of manual editing	String

Information is included regarding whether the adjacent ice margin is either the ice sheet or PGIC ("margin", Table 2). This margin information originates from the MEaSUREs GIMP 15 m ice mask, previously used for the spatial filtering. In addition, each ice-marginal lake is assigned a region – north-west (NW), north (NO), north-east (NE), central-east (CE), south-east (SE), south-west (SW), and central-west (CW) ("region", Table 2). These regions and their corresponding names are based on ice sheet catchment regions from Mouginot and Rignot (2019), which are used to also extend to the terrestrial periphery beyond the ice sheet. By doing so, regional trends can be identified from ice-marginal lakes with a PGIC margin as well as the ice sheet (Carrivick et al., 2023).

Lake names ("lake_name", Table 2) are assigned in instances where a name is available, with preference to New Greenlandic (Kalaallisut) placenames followed by Old Greenlandic and

alternative foreign placenames. Placenames are provided by the Oqaasileriffik (Language Secretariat of Greenland) placename database, filtering placenames to those associated with lake features. The Oqaasileriffik placename database is distributed with QGreenland v3.0 (Moon et al., 2023).

A readme file is included with the dataset that outlines the data file contents and terms of use. An additional data file is included which is a point vector shapefile representing all identified lakes across the inventory series (presented in Figure 1). This includes manually identified lake locations that are not captured in the inventory series using the automated classification approaches.

3. Methodology

3.1. Lake classification

Lake classifications are based on those adopted in the production of the 2017 Greenland ice-marginal lake inventory, which is summarised in Figure 4 (How et al., 2021). The main progression (and therefore difference) is that the processing pipeline is now unified and operates through Google Earth Engine to conduct the heavy image processing (How, 2024), and filtering/post-processing conducted with open-source spatial packages in Python, namely geopandas (Kelsey et al., 2020) and rasterio (Gillies et al., 2013). The Python pipeline is deployable as a package called GrIML (How, 2024; How et al., In prep), which is accompanied by thorough documentation and guidelines on its use (at https://griml.readthedocs.io). This ensures a high level of reproducibility and transparency that adheres to the FAIR (Findability, Accessibility, Interoperability, and Reusability) principles (Wilkinson et al., 2016).

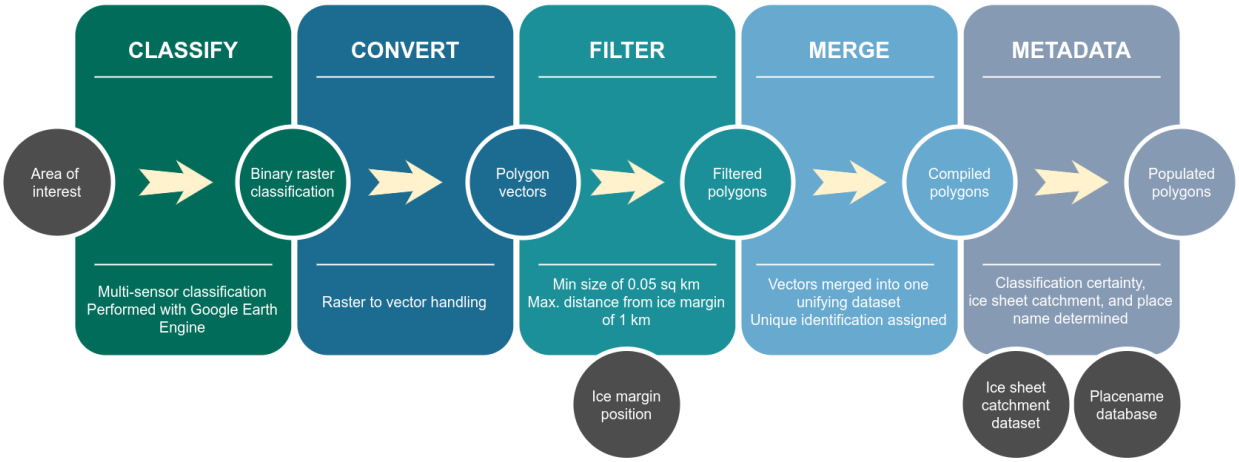

Figure 4: A visualisation of the processing workflow for the generation of the ice-marginal lake inventory series, including components performed with Google Earth Engine ("Classify") and the Python package GrIML (How, 2024), which utilises Python spatial data handling packages geopandas (Kelsey et al., 2020) and rasterio (Gillies et al., 2013). The workflow is based on How et al. (2021). The annotated rectangles refer to process stages (reading from left to right), the coloured annotated circles represent intermediary outputs to the corresponding process stages in the workflow, and the grey annotated circles represent workflow inputs.

3.1.1. SAR backscatter classification

Water bodies are classified from Sentinel-1 GRD scenes, which are dual-polarization C-band SAR images (Table 1). Scenes are pre-processed using the Sentinel-1 Toolbox to generate calibrated, ortho-corrected data, specifically thermal noise removal, radiometric calibration and terrain correction using either the SRTM 30 or ASTER DEM. Scenes are then filtered to IW swath and HH polarisation, with image acquisitions limited to the summer months (1 July to 31 August) of each inventory year (2016 to 2023). Averaged mosaics for each year are derived from all summer scenes for each year of the inventory series at a 10 m spatial resolution. These mosaics are smoothed using a focal median of 50 metres. Classifications are derived from these averaged and smoothed mosaics using a static threshold trained for detecting open water bodies (How et al., 2021).

3.1.2. Multi-spectral indices classification

Water bodies are classified from Sentinel-2 MSI, TOA, Level-1C scenes acquired for the summer months (1 July to 31 August) of each inventory year (2016 to 2023) (Table 1). Clouds are masked using the cloud mask provided with each scene (QA60), masking out opaque and cirrus clouds. The bands of interest are extracted, specifically blue (B2), green (B3), red (B4), near-infrared (B8), and the two shortwave infrared bands (B11, B12). The shortwave infrared bands are resampled from 60 m to 10 m spatial resolution, and then averaged band mosaics are produced from all summer scenes for each inventory year.

Five spectral indices are used to classify open water bodies: 1) Normalised Difference Water Index (NDWI) (McFeeters, 1996); 2) Modified Normalised Difference Water Index (MNDWI) (Xu, 2006); 3) Automated Water Extraction Index (with shadow) (AWEI) (Feyisha et al., 2014); 4) Automated Water Extraction Index (no shadow) (AWEInsh) (Feyisha et al., 2014); 5) Snow brightness radio (BRIGHTNESS):

$$NDWI = \frac{(B3 - B8)}{(B3 + B8)}$$

$$MNDWI = \frac{(B3 - B11)}{(B3 + B11)}$$

$$AWEIsh = B2 + 2.5 \cdot B3 - 1.5 \cdot (B8 + B11) - 0.25 \cdot B12$$

$$AWEInsh = 4 \cdot (B3 - B11) - (0.25 \cdot B8 + 2.75 \cdot B12)$$

$$BRIGHTNESS = \frac{(B4 + B3 + B2)}{3}$$

Each spectral index (NDWI, MNDWI, AWEIsh, AWEInsh and BRIGHTNESS) has specific targets, namely shadow on water, snow/ice in water, sediment-loaded water with shadowing, optimised sediment-loaded water without shadowing, and snow-covered areas, respectively. Thresholds for the indices are chosen based on previous studies of ice-marginal lakes (How et al., 2021; Shugar et al., 2020), where positive classifications adhere to all thresholds.

3.1.3. Sink classification

Water bodies are classified from the ArcticDEM 2-metre mosaic (version 3), which is compiled from the best quality ArcticDEM strip files and manually adjusted to form a static data product (Table 1). The mosaic is smoothed using a focal median of 110 metres, and DEM depressions (i.e. where water pools) are filled over a 50-pixel moving window and subsequently subtracted from the original mosaic; producing the outline of a lake. It is noted that this is an indirect water classification method compared to the former two approaches (which directly detect water). Therefore, validation is required to confirm the presence of water in classified DEM sinks, which will be elaborated further in the following subsection.

3.2. Summer surface water temperature estimation

A summer surface water temperature estimate is provided with each classified lake across inventory years. Surface water temperature estimates are derived from the Landsat 8 and Landsat 9 OLI/TIRS surface temperature data, which is a Collection 2, Level-2 science product that is part of a large Landsat re-processing effort (Table 1). Surface temperature estimates are generated from descending, day-lit Landsat 8/9 acquisitions with thermal infrared band information (30-metre spatial resolution) and auxiliary data (i.e. Top Of Atmosphere reflectance and brightness temperature), along with ASTER datasets (global emissivity and normalised difference vegetation index) and atmospheric data (geopotential height, specific humidity and air temperature) (Earth Resources Observation and Science (EROS) Center, 2020; Malakar et al., 2020).

Surface temperature values (LSTscaled) are corrected to surface water temperature (LSTwater) using the following calibration:

$$LST_{scaled} = LST_{land} \times 0.00341802 + 149.0$$

$$LST_{water} = (0.806 \times LST_{scaled} + 54.37) - 273.15$$

Where LSTscaled is the applied scale factor for computing temperature in Kelvin (K) units, and LSTwater is the calibrated surface water temperature in degrees Celsius (NASA Applied Remote Sensing Training (ARSET) program, 2022; Dyba et al., 2022). This calibration has previously shown strong correlations against in situ measurements (RMSE = 3.68°C and R^2 = 0.8) from 38 lakes in Poland, highlighting accurate estimates through a simple linear calibration (Dyba et al., 2022).

A summer average surface water temperature estimate is derived using this approach for each lake extent in the ice-marginal lake inventory series. Scenes are filtered by a maximum cloud cover of 20%, with acquisitions limited to the month of August to reduce the probability of ice-covered lake conditions. Lake extents are reduced by a border pixel (i.e. 30 metres) to reduce the impact of edge effects. An average, maximum and minimum surface water temperature value is computed for each lake extent over each inventory year, along with the standard deviation.

4. Data Quality and Validation

4.1. Data Quality Control

Identified water bodies (using the three classified approaches) are compiled for each inventory year and filtered via three strategies: 1) by location; 2) by size; 3) by manual curation (Figure 4). Firstly, lakes are filtered based on their location relative to the ice margin. Here, a 1 km buffer is derived around the MEaSUREs GIMP 15 m ice mask and classified water bodies are retained if they are located within the buffer (Howat, 2017; Howat et al., 2014). Classified water bodies are filtered by size, only retaining lakes above a minimum size threshold of 0.05 km^2; as adopted by How et al. (2021). Finally, each inventory year dataset is manually curated to remove misclassifications, edit classifications (for example, where the shadowing mask does not adequately remove shadowing effects), remove detected water bodies that do not hold water in specific years, and remove water bodies that are detached from the ice margin. This manual curation is carried out via visual inspection of Sentinel-2 TOA Level-1C true colour composites from each inventory year.

4.2. Lake abundance error estimation

Previous error analysis suggested that the 2017 ice-marginal lake inventory captured 92% of lake abundance, based on comparison between the inventory and user-defined lakes over four regions at the NE, NW and SW ice sheet margin, and a region within the PGICs, covering a collective area of 40,000 km^2. This formed an error estimate for lake abundance of ±8% (see How et al., 2021, for more details). As a follow-on to this effort, ice-marginal lakes are manually verified for each inventory year, including those that were not classified using the automated methods. Across all inventory years, 4543 ice-marginal lakes have been manually identified in total, of which 2915 (64%) are present in the ice-marginal lake inventory series. This forms a revised lake abundance error estimation of ±36%. This error estimation is substantially different from the former estimate because the 2017 ice-marginal lake inventory included manual lake delineations, whereas the inventory series presented here only includes automated classifications (i.e. no manual lake delineations are included).

4.3. Surface lake temperature error estimation

Surface water temperature estimates are validated against existing in situ measurements of lake temperature in Greenland (Fig. 5). The only known, open-access, long-term in situ measurements are from Kangerluarsunnguup Tasia (also known as Badesø, 64°07’50”N, 51°21’36”W) and Qassi-Sø (64°09’14”N, 51°18’27”W), two small valley lakes at the bottom of Kobbefjord, near Nuuk in southwest Greenland. The Kobbefjord catchment area is an intensive monitoring site that is part of the Greenland Ecosystem Monitoring (GEM) programme (https://g-e-m.dk). Water measurements have been collected from Kangerluarsunnguup Tasia and Qassi-sø since 2008; such as conductivity, acidity (pH) and water temperature. Water temperature measurements have been taken at fixed depths of 2 m and 10 m (GEM BioBasis, 2024).

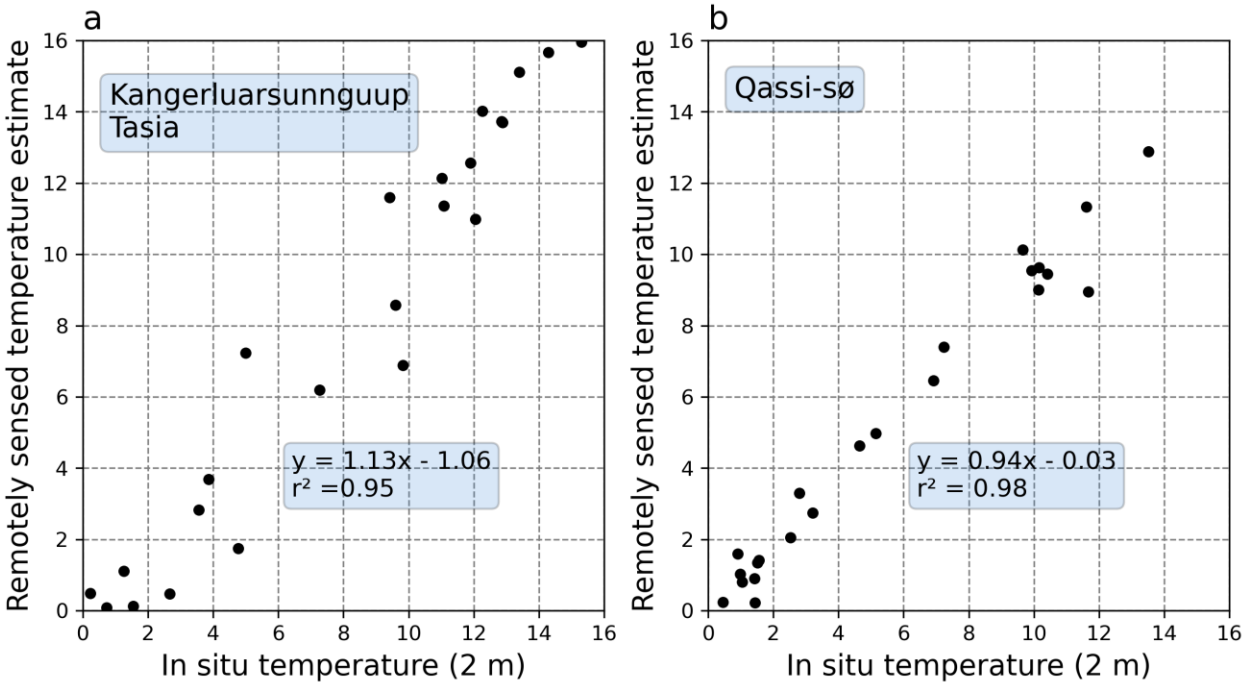

Figure 5: Comparison of in situ surface (2 m) water temperature measurements (from GEM BioBasis) with remotely sensed temperature estimates from Kangerluarsunnguup Tasia (a) and Qassi-Sø (b). Both sites demonstrate a strong correlation, with values at Kangerluarsunnguup Tasia and Qassi-Sø exhibiting a correlation (r-squared value) of 0.95 and 0.98, respectively.

Comparison of the 2 m water temperature measurements with those estimated using the remote sensing approach adopted here exhibit a strong correlation (>0.9), with an RMSE of 1.45 (, Kangerluarsunnguup Tasia) and 0.78 (Qassi-Sø), suggesting that the remotely sensed temperature estimates are reliable (Figure 5). Estimates from Kangerluarsunnguup Tasia slightly over-predict measured temperatures, whilst they are under-predicted at Qassi-sø, equating to an average difference of 1.21°C and 0.55°C, respectively. An error estimation of ±0.88°C is determined, based on the average difference from all data points across the two lake sites.

5. Data Availability

The dataset is openly available on the GEUS Dataverse, including a cite-able DOI, at https://doi.org/10.22008/FK2/MBKW9N (How et al., 2024). If the dataset is presented or used to support results of any kind then we ask that a reference to the dataset be included in publications, along with any relevant publications from the data production team. If the dataset is crucial to the main findings of a publication, then we ask for a member of the data production team to be included as a co-author.

The production code for making the inventory series is openly available at https://github.com/GEUS-Glaciology-and-Climate/GrIML with a cite-able DOI (How, 2024). It is distributed as a deployable, version-controlled and peer-reviewed Python package (How et al., In

prep). If the production code is used or adapted, then we ask for a reference to the peer reviewed paper to be included in publications.

6. Potential Applications and Future Updates

6.1. Uses for the ice-marginal lake inventory series

The inventory series presented here is the first step to quantify the terrestrial storage of meltwater, and how it changes over time, which would be highly valuable for refining estimations of the future sea level contribution of the Greenland Ice Sheet and surrounding PGICs.

The ice-marginal lake inventory series is applicable to climate and cryosphere research, enabling inter-annual comparison of lake change (abundance, extent and surface temperature) over time, similar to inventories for other regions such as Svalbard (Wieczorek et al., 2023). Such inventories have been used to characterise ice dam types (e.g. Rick et al., 2022), monitor GLOFs (e.g. Lützow, Veh and Korup, 2023), and assess lake conditions in catchments of interest (e.g. Hansen et al., In Review). Lake conditions could also provide insights into glacier dynamics in lacustrine settings around Greenland, for example, to investigate submarine melting in lacustrine settings and its impact on glacier retreat (e.g. Mallalieu et al., 2021).

Beyond scientific research, the inventory series could also be a useful resource in Greenland's assessment of infrastructure, with hydropower being the main sector that could benefit. Given Greenland's commitment to the Paris Agreement strongly suggests the expansion of current hydropower infrastructure, the ice-marginal lake inventory series could be valuable in infrastructure assessments (Naalakkersuisut, 2023). For example, the inventory series can be used to distinguish glacier-fed lakes from catchment-fed lakes, identify draining lakes, and other characteristics that are useful to discern viable catchment regions.

6.2. The future of the ice-marginal lake inventory series

It is planned to update the ice-marginal lake inventory series annually with new inventory years, using the methodology and data sources outlined here. A possibility could be to also include past years, prior to the Sentinel satellite era, however, this is limited by the open availability of SAR and multi-spectral satellite imagery at a high spatial resolution (i.e. 10 metres). Another avenue to explore is the inclusion of manually delineated lake extents where lakes have not been identified with the automated classification approaches. However, this would add further labour to the manual curation of the inventory series. An alternative would be to look at implementing new automated classification methods with machine learning, using the existing lake classifications as the foundation of a training dataset. Lake classification aided by machine learning has been successfully used for supraglacial lake detection on the Greenland Ice Sheet, so the use of machine learning in ice-marginal lake detection is likely to be feasible (Lutz et al., 2023; Melling et al., 2024).

One of the key limitations of this work to be addressed in the future is the reliance on static data products, in particular the static ArcticDEM 2 m mosaic for classification, and the MEaSUREs

GIMP static ice margin for filtering. The use of static data products in the inventory series presented here highlights the importance of high-labour, time-consuming manual dataset curation. For the DEM classification, an alternative would be the ArcticDEM strip data product, which is time variant, but data coverage is lacking currently and scenes covering all Greenland are not possible from year to year. Another option would be to use coarser spatial resolution DEM products, such as PRODEM (500 m) (Winstrup, 2023), however, smaller lakes would not be identifiable. For the ice margin filtering, machine learning ice margin products show promise in being used in future editions of the inventory series, such as AutoTerm (trained with the TeamPicks dataset) (Goliber et al., 2022; Zhang, E. et al., 2023). The use of dynamic ice margin datasets in the future could negate the need for generating a classification spatial buffer around the margin data, and instead classify ice-marginal lakes directly from their intersection with the ice margin position.

Another opportunity to further the inventory series would be the addition of valuable metadata on the characteristics and dynamics of each classified ice-marginal lake. The type of damming has been included in other inventories, proving to be useful for assessing present and future lake conditions under a changing climate (e.g. Rick et al., 2022). Incorporating known GLOFs and/or drainage periods for each lake would also provide insight into abrupt changes in terrestrial water storage and be highly valuable information for infrastructure assessments, such as hydropower utilities (e.g. Domsgaard et al., 2024).

7. Conclusions

Here, a series of annual inventories are presented that represent ice-marginal lake abundance, surface area extents, and surface temperature estimates across Greenland for the years 2016 to 2023. Ice-marginal lakes are mapped across the margin of the Greenland Ice Sheet and its surrounding PGICs The dataset demonstrates lake change over the 8-year period, which can be assessed at various scales, from individual lake, to regional, to Greenland-wide change. The annual ice-marginal lake inventory series is openly available on the GEUS Dataverse with a cite-able DOI at https://doi.org/10.22008/FK2/MBKW9N, including supporting metadata and documentation (How et al., 2024).

With each year, a new addition will be added to this dataset, with the hope that the inventory series could be used in the future to assess lake change at multi-decadal time scales. This is supported by GrIML, an open processing workflow with open-source programming that is accessible to novice programmers with thorough documentation and straightforward deployment (How, 2024; How et al., In Prep).

The annual ice-marginal lake inventory series is a valuable addition to addressing current limitations in terrestrial water storage and its influence on Greenland's future sea level contribution. This dataset is the first step towards quantifying meltwater storage at the margins of the Greenland Ice Sheet, and surrounding PGICsp It also provides insight into lake change over time, and the resulting impact on glacier dynamics, such as lacustrine frontal ablation (i.e. submarine melting and calving). Beyond the cryospheric science community, the dataset will be invaluable to related

disciplines in biology and ecology, where changes in lake conditions shape Arctic ecosystems and biological activity. On a national level, the inventory series could be a useful resource in environmental management and infrastructure assessment, for instance in the expansion of hydropower utilities as suggested in Greenland's new commitments to the Paris Agreement.

8. Acknowledgements

This work was supported by an ESA (European Space Agency) Living Planet Fellowship (4000136382/21/I-DT-lr) entitled "Examining Greenland's Ice Marginal Lakes under a Changing Climate". Further support was provided by PROMICE, funded by the Geological Survey of Denmark and Greenland (GEUS) and the Danish Ministry of Climate, Energy and Utilities under the Danish Cooperation for Environment in the Arctic (DANCEA), conducted in collaboration with DTU Space (Technical University of Denmark) and Asiaq Greenland Survey. In situ lake temperature datasets are supported by BioBasis under the Greenland Ecosystem Monitoring Programme (GEM). Additional thanks to Stephen Plummer and Marcus Engdahl for technical advice and support, and Sikkersoq Olsen from Oqaasileriffik (the Language Secretariat of Greenland) for clarification on the Kalaallisut terminology for GLOFs.

9. References

AMAP (2021) Arctic Climate Change Update 2021: Key Trends and Impacts. Summary for Policy-makers. Arctic Monitoring and Assessment Programme (AMAP), Tromsø, Norway. 16 pp

Andreassen LM, Nagy T, Kjøllmoen B, Leigh JR. (2022) An inventory of Norway's glaciers and ice-marginal lakes from 2018–19 Sentinel-2 data. Journal of Glaciology. 68(272):1085-1106. doi:10.1017/jog.2022.20

Carrivick, J. L. & Quincey, D. J. (2014) Progressive increase in number and volume of ice-marginal lakes on the western margin of the Greenland Ice Sheet. Glob. Planet. Change 116, 156–163

Carrivick, J. L. and Tweed, F. S. (2016) A global assessment of the societal impacts of glacier outburst floods. Global and Planetary Change 144, 1-16. https://doi.org/10.1016/j.gloplacha.2016.07.001

Carrivick, J. L. and Tweed, F. S. (2019) A review of glacier outburst floods in Iceland and Greenland with a megafloods perspective. Earth-Science Reviews 196, 102876. https://doi.org/10.1016/j.earscirev.2019.102876

Carrivick JL, Tweed FS, Ng F, Quincey DJ, Mallalieu J, Ingeman-Nielsen T, Mikkelsen AB, Palmer SJ, Yde JC, Homer R, Russell AJ and Hubbard A (2017) Ice-Dammed Lake Drainage Evolution at Russell Glacier, West Greenland. Front. Earth Sci. 5:100. doi: 10.3389/feart.2017.00100

Carrivick, J. L. et al. (2022) Ice-marginal proglacial lakes across Greenland: present status and a possible future. Geophys. Res. Lett. 49, e2022GL099276

Chen, F., Zhang, M., Guo, H., Allen, S., Kargel, J. S., Haritashya, U. K., and Watson, C. S.: Annual 30 m dataset for glacial lakes in High Mountain Asia from 2008 to 2017, Earth Syst. Sci. Data, 13, 741–766, https://doi.org/10.5194/essd-13-741-2021, 2021.

Dye, A. et al. (2021) Warm Arctic Proglacial Lakes in the ASTER Surface Temperature Product. Remote Sensing 13(15), 2987. https://doi.org/10.3390/rs13152987

Dømgaard, M., Kjeldsen, K. K., Huiban, F., Carrivick, J. L., Khan, S. A., and Bjørk, A. A. (2023) Recent changes in drainage route and outburst magnitude of the Russell Glacier ice-dammed lake, West Greenland, The Cryosphere, 17, 1373–1387, https://doi.org/10.5194/tc-17-1373-2023

Dømgaard, M., Kjeldsen, K., How, P. et al. (2024) Altimetry-based ice-marginal lake water level changes in Greenland. Commun. Earth Environ. 5, 365. https://doi.org/10.1038/s43247-024-01522-4

Earth Resources Observation and Science (EROS) Center. (2020). Landsat 8-9 Operational Land Imager / Thermal Infrared Sensor Level-2, Collection 2 [dataset]. U.S. Geological Survey. https://doi.org/10.5066/P9OGBGM6

Feyisa, G. L., Meilby, H., Fensholt, R. & Proud, S. R. Automated Water Extraction Index: A new technique for surface water mapping using Landsat imagery. Remote Sens. Environ. 140, 23–35. https://doi.org/10.1016/j.rse.2013.08.029 (2014).

Gillies, S. et al. (2013) Rasterio: geospatial raster I/O for Python programmers. https://github.com/rasterio/rasterio

Goliber, S., Black, T., Catania, G., Lea, J. M., Olsen, H., Cheng, D., Bevan, S., Bjørk, A., Bunce, C., Brough, S., Carr, J. R., Cowton, T., Gardner, A., Fahrner, D., Hill, E., Joughin, I., Korsgaard, N. J., Luckman, A., Moon, T., Murray, T., Sole, A., Wood, M., and Zhang, E. (2022) TermPicks: a century of Greenland glacier terminus data for use in scientific and machine learning applications, The Cryosphere, 16, 3215–3233, https://doi.org/10.5194/tc-16-3215-2022

Grinsted, A., Hvidberg, C.S., Campos, N. et al. (2017) Periodic outburst floods from an ice-dammed lake in East Greenland. Sci Rep 7, 9966. https://doi.org/10.1038/s41598-017-07960-9

Greenland Ecosystem Monitoring (2024) BioBasis Nuuk - Lakes - Temperature in lakes (Version 1.0). [Data set] [CC-BY-SA-4.0]. Greenland Ecosystem Monitoring. https://doi.org/10.17897/BKTY-J070

Holt, E., Nienow, P., Medina-Lopez, E. (2024) Terminus thinning drives recent acceleration of a Greenlandic lake-terminating outlet glacier. Journal of Glaciology. 1-13. doi:10.1017/jog.2024.30

How, P. (2024) PennyHow/GrIML v0.1.0. Zenodo. https://doi.org/10.5281/zenodo.11395471

How, P., Messerli, A., Mätzler, E., Santoro, M., Wiesmann, A., Caduff, R., Langley, K., Bojesen, M. H., Paul, F., Kääb, A. and Carrivick, J. L. (2021) Greenland-wide inventory of ice marginal lakes

using a multi-method approach. Scientific Reports 11, 4481. https://doi.org/10.1038/s41598-021-83509-1

How, P. et al. (2024) "Greenland Ice Marginal Lake Inventory annual time-series Edition 1" [dataset], GEUS Dataverse, https://doi.org/10.22008/FK2/MBKW9N

Howat, I. MEaSUREs Greenland Ice Mapping Project (GIMP) land ice and ocean classification mask, version 1 [GimpIceMask 15 m tiles 0-5]. NASA National Snow and Ice Data Center Distributed Active Archive Center, Boulder, Colorado USA. https://doi.org/10.5067/B8X58MQBFUPA (2017).

Howat, I. M., Negrete, A. & Smith, B. E. The Greenland Ice Mapping Project (GIMP) land classification and surface elevation data sets. Cryosphere 8, 1509–1518. https://doi.org/10.5194/tc-8-1509-2014 (2014).

Kelsey, J. et al. (2020) geopandas/geopandas: v0.8.1. https://doi.org/10.5281/zenodo.394676

Kjeldsen, K. K. et al. Ice-dammed lake drainage cools and raises surface salinities in a tidewater outlet glacier fjord, west Greenland. J. Geophys. Res. Earth Surf. 119, 1310–1321. https://doi.org/10.1002/2013JF003034 (2014)

Kjeldsen, K. K. et al. (2017) Ice-dammed lake drainage in west Greenland: Drainage pattern and implications on ice flow and bedrock motion. Geophys. Res. Lett. 44(14), 7320-7327. https://doi.org/10.1002/2017GL074081

Lutz, K.; Bahrami, Z.; Braun, M. Supraglacial Lake Evolution over Northeast Greenland Using Deep Learning Methods. Remote Sens. 2023, 15, 4360. https://doi.org/10.3390/rs15174360

Lützow, N., Veh, G., and Korup, O. (2023) A global database of historic glacier lake outburst floods, Earth Syst. Sci. Data, 15, 2983–3000, https://doi.org/10.5194/essd-15-2983-2023

McFeeters, S. K. The use of the Normalized Difference Water Index (NDWI) in the delineation of open water features. Int. J. Remote Sens. 17, 1425–1432. https://doi.org/10.1080/01431169608948714 (1996).

Malakar, N. K., G. C. Hulley, S. J. Hook, K. Laraby, M. Cook and J. R. Schott, "An Operational Land Surface Temperature Product for Landsat Thermal Data: Methodology and Validation," in IEEE Transactions on Geoscience and Remote Sensing, vol. 56, no. 10, pp. 5717-5735, Oct. 2018, doi: 10.1109/TGRS.2018.2824828.

Mallalieu, J., Jonathan L. Carrivick, Duncan J. Quincey, Cassandra L. Raby (2021) Ice-marginal lakes associated with enhanced recession of the Greenland Ice Sheet. Global and Planetary Change 202, 103503. https://doi.org/10.1016/j.gloplacha.2021.103503

Melling, L., Leeson, A., McMillan, M., Maddalena, J., Bowling, J., Glen, E., Sandberg Sørensen, L., Winstrup, M., and Lørup Arildsen, R.: Evaluation of satellite methods for estimating supraglacial

lake depth in southwest Greenland, The Cryosphere, 18, 543–558, https://doi.org/10.5194/tc-18-543-2024, 2024.

Moon, T. A., M. Fisher, T. Stafford, and A. Thurber (2023). QGreenland (v3) [dataset], National Snow and Ice Data Center. https://doi.org/10.5281/zenodo.12823307

Mouginot, J. and Rignot, E. Glacier catchments/basins for the Greenland Ice Sheet. 4137543 bytes. Dryad https://doi.org/10.7280/D1WT11 (2019).

Naalakkersuisut (2023) Impact Analysis of the Paris Agreement on Greenlandic Society. https://naalakkersuisut.gl/-/media/horinger/2023/02/0602_parisaftale/eng-hovedrapport--konsekvensanalyse-af-parisaftalen-for-det-grnlandske-samfund.pdf [accessed 01.11.2024]

NASA Applied Remote Sensing Training (ARSET) program (2022) ARSET Training: Satellite Remote Sensing for Measuring Urban Heat Islands and Constructing Heat Vulnerability Indices. https://code.earthengine.google.com/7103291d8b113cd38e573f2e3a67bb51 [accessed 02.12.2024]

Rick, B., McGrath, D., Armstrong, W., and McCoy, S. W. (2022) Dam type and lake location characterize ice-marginal lake area change in Alaska and NW Canada between 1984 and 2019, The Cryosphere, 16, 297–314, https://doi.org/10.5194/tc-16-297-2022

Rick, B., McGrath, D., McCoy, S.W. et al. Unchanged frequency and decreasing magnitude of outbursts from ice-dammed lakes in Alaska. Nat Commun 14, 6138 (2023). https://doi.org/10.1038/s41467-023-41794-6

Shugar, D. H., Burr, A., Haritashya, U.K. Kargel, J. S., Scott Watson, C., Kennedy, M. C., Bevington, A. R., Betts, R. A., Harrison, S. and Strattman, K. (2020) Rapid worldwide growth of glacial lakes since 1990. Nat. Clim. Chang. 10, 939–945. https://doi.org/10.1038/s41558-020-0855-4

Styrelsen for Dataforsyning and Infrastruktur (2024) Sentinel2 10m 2022 mosaic. In: Satellitfoto Grønland. https://dataforsyningen.dk/data/4783 [accessed 02.12.2024]

Sutherland, J. L., J. L. Carrivick, N. Gandy, J. Shulmeister, D. J. Quincey, S. L. Cornford (2020) Proglacial Lakes Control Glacier Geometry and Behavior During Recession. Geophys. Res. Lett. 47(19) e2020GL088865. https://doi.org/10.1029/2020GL088865

Veh, G., Lützow, N., Tamm, J. et al. Less extreme and earlier outbursts of ice-dammed lakes since 1900. Nature 614, 701–707 (2023). https://doi.org/10.1038/s41586-022-05642-9

Wieczorek I, Strzelecki MC, Stachnik Ł, Yde JC, Małecki J. Post-Little Ice Age glacial lake evolution in Svalbard: inventory of lake changes and lake types. Journal of Glaciology. 2023;69(277):1449-1465. doi:10.1017/jog.2023.34

Wiesmann, A.; Santoro, M.; Caduff, R.; How, P.; Messerli, A.; Mätzler, E.; Langley, K.; Høegh Bojesen, M.; Paul, F.; Kääb, A.M. (2021): ESA Glaciers Climate Change Initiative (Glaciers_cci): 2017 inventory of ice marginal lakes in Greenland (IIML), v1. Centre for Environmental Data

Analysis, 19 February 2021. doi:10.5285/7ea7540135f441369716ef867d217519. https://dx.doi.org/10.5285/7ea7540135f441369716ef867d217519

Winstrup, M., Ranndal, H., Larsen, S. H., Simonsen, S. B., Mankoff, K. D., Fausto, R. S., and Sørensen, L. S. (2023) PRODEM: Annual summer DEMs (2019–present) of the marginal areas of the Greenland Ice Sheet, Earth Syst. Sci. Data Discuss. [preprint], https://doi.org/10.5194/essd-2023-224, in review.

Xu, H. Modification of normalised difference water index (NDWI) to enhance open water features in remotely sensed imagery. Int. J. Remote Sens. 27, 3025–3033. https://doi.org/10.1080/01431160600589179 (2006).

Zhang, E., Catania, G., and Trugman, D. T. (2023) AutoTerm: an automated pipeline for glacier terminus extraction using machine learning and a “big data” repository of Greenland glacier termini, The Cryosphere, 17, 3485–3503, https://doi.org/10.5194/tc-17-3485-2023

Zhang, G., Bolch, T., Yao, T. et al. Underestimated mass loss from lake-terminating glaciers in the greater Himalaya. Nat. Geosci. 16, 333–338 (2023). https://doi.org/10.1038/s41561-023-01150-1

Zhang, G., Carrivick, J.L., Emmer, A. et al. Characteristics and changes of glacial lakes and outburst floods. Nat Rev Earth Environ 5, 447–462 (2024). https://doi.org/10.1038/s43017-024-00554-w